Estimating Polymer/Solvent Diffusion Coefficient by Optimization Procedure

Frédéric Doumenc and Béatrice Guerrier
Lab. FAST (Université Pierre et Marie Curie—Université Paris Sud—CNRS), 91405 Orsay, FRANCE

Solvent diffusion in polymer solutions is one of the main parameters that determine the drying kinetics of polymer films, especially in the concentrated domain. As is well known for polymer/solvent solutions, solvent diffusion coefficients decrease by several orders of magnitude when the solvent concentration decreases. Direct measurements of these coefficients are complex and time-consuming, and most often dedicated to well-characterized ''model'' systems. In this study, another approach is developed that is based on simple gravimetric experiments coupled with the modelization of the drying kinetics and an optimization iterative procedure. The sensitivity of the method to various errors (measurement errors and uncertainties on a priori known parameters) is thoroughly investigated. The method accurately estimates diffusion coefficients on a large concentration domain, provided a suitable experimental strategy is used.

Introduction

Numerous theoretical and experimental works are dedicated to the analysis of the variation of diffusion coefficients with solvent concentration (Neogi, 1996). However, direct measurements of these coefficients are complex and time-consuming, and most often dedicated to well-characterized ''model'' systems. Among those various experimental methods, one can cite solvent self-diffusion measurements using nuclear magnetic resonance (Blum and Pickup, 1987; Waggoner et al., 1993; Bandis et al., 1995), or probe diffusion measurements using various techniques: forced Rayleigh scattering (Lodge et al., 1990; Frick et al., 1990; Lohfink and Sillescu, 1993; Zielinski et al., 1995), techniques involving fluorescence nonradiative energy transfer (Deppe et al., 1996) or Taylor dispersion and phosphorescence quenching (Wisnudel and Torkelson, 1996).

Depending on the concentration domain, several theoretical approaches have been proposed (Waggoner et al., 1993), among which are the framework of the scaling laws for semidilute solutions (de Gennes, 1979), and the free-volume theory for solvent self-diffusion (Zielinski, 1996; Vrentas and Vrentas, 1998). Experimental data of solvent self-diffusion coefficients have been successfully described by free-volume models, for various systems (Pickup and Blum, 1989; Waggoner et al., 1993; Hong et al., 1997). However, several physicochemical parameters are needed to obtain quantitative estimations with these models, which limit their use to well-characterized systems. Moreover, since we are interested in the drying of polymer films, the parameter that characterizes solvent desorption is the solvent/polymer mutual-diffusion coefficient, D_{SP}. No general relationship between self- and mutual-diffusion coefficients is currently available and validated on the whole concentration domain, though some approximated relations have been developed (Vrentas and Vrentas, 1993, 1998).

Given these difficulties, it is not possible to get a good estimation of mutual-diffusion coefficients from the literature as soon as complex systems are considered. For example, industrial varnishes are always a blend of several polymers or copolymers, and are not necessarily well characterized (Bouchard et al., 1998). The aim of this study is to develop an estimation approach to get the mutual-diffusion coefficient of complex solutions. (We make the assumption that the polymers under study are miscible, and that it makes sense for a given blend to define a solvent/polymers mutual-diffusion coefficient that depends only on temperature and solvent concentration in the rubbery domain.) Multisolvents are not considered here (Zielinski and Hanley, 1999). The proposed method is based on a simple drying experiment, coupled with a process modelization and an optimization approach. The methodology and the different optimization steps

Correspondence concerning this article should be addressed to F. Doumenc.

are described in the following section. Since we study the feasibility and robustness of the proposed estimation procedure, we do not use real experimental data but virtual ones. They are obtained thanks to the numerical simulation of test problems. These test problems are given in the third section, together with a short description of a typical drying kinetics. The fourth section is devoted to the definition of the experimental strategy, that is, the choice of a given set of experiments, that brings enough information for the estimation of the mutual-diffusion coefficient. In the last section, the method accuracy and robustness are investigated.

Estimation Method

Experimental procedure

As was said in the Introduction, this article deals with a feasibility study of the estimation method and is not dedicated to a detailed presentation of the experiments. We just give some general characteristics of the experimental procedure. We are looking for experiments that are easy to perform, but of course sensitive to the property we are interested in. Previous studies have shown that simple evaporation experiments in ambient air, with continuous recording of the mass evolution of the polymer solution, are suitable for our propose: indeed, the mass evolution is sensitive to the physicochemical parameters of the polymer solutions, and especially to mutual-diffusion coefficient (Guerrier et al., 1998). These preliminary results have been obtained with a precise balance (resolution of 10^{-4} g). The semidiluted solution is placed in a dish large enough to neglect boundary effects, with an initial thickness of a few millimeters. Since experiments are performed at room temperature and since the evaporation flux is not very important, evaporative cooling was shown to be less than a few degrees. As a consequence, the variation of D_{SP} with temperature is neglected. Let us emphasize that these simple gravimetric experiments do not compare with sophisticated differential sorption gravimetric experiments in a pressure-controlled chamber that use microbalance (Billovits and Durning, 1993; Bouchard et al., 1998). The drawback of this simple experimental procedure is to give a global measurement that is integrated on the whole film thickness. Since important concentration gradients appear during the film drying (Guerrier et al., 1998), it is not possible to estimate $D_{SP}(\omega_S)$ directly from the mass evolution (where ω_S is the solvent weight fraction). An estimation approach, using the modelization of the drying kinetics, is needed.

Optimization

The mutual-diffusion coefficient is obtained by an iterative procedure, with the following steps: a first arbitrary initial estimation $D_{SP_0}(\omega_S)$ is chosen. This estimation is used to calculate the mass evolution, thanks to a model of the drying process. A criterion is calculated that evaluates the distance between experimental and calculated mass on the whole time horizon. Then an optimization algorithm leads to a new estimation of $D_{SP}(\omega_S)$ that reduces the criterion value. The entire procedure is then started again, until convergence. Given this general framework, we detail some specific points in the following.

Parameterization. A continuous expression of the unknown function $D_{SP}(\omega_S)$ is needed by the drying model. Two different parameterizations have been used in our study. The first one uses cubic splines. The interpolation points are irregularly distributed: the interval magnitude decreases with ω_S according to a geometric progression. The proportion of the geometric progression and the number of intervals have been chosen in order to get a negligible error between the original function $D_{SP}(\omega_S)$ of our virtual test problem and its parameterization.

Eight intervals are used in our study, and then we face an optimization problem with nine unknown parameters, p_i ($0 \le i \le 8$), where p_i is the decimal logarithm of D_{SP} at the ith interpolation point (with increasing i for increasing ω_S). The function $D_{SP}(\omega_S)$ and the definition of the nine interpolation points are given in Figure 1 (continuous line) and Table 1.

The second parameterization uses a model based on the free-volume theory to get $D_{\text{self}}(\omega_S)$ (solvent self-diffusion coefficient) coupled with a model expressing $D_{SP}(\omega_S)$ from $D_{\text{self}}(\omega_S)$ (Vrentas and Vrentas, 1998). As previously said, it is most often impossible to get all the physical parameters required by these models, so that in the estimation procedure we only use the shape of the functions $D_{\text{self}}(\omega_S)$ and $D_{SP}(\omega_S)$, which leads to a five-parameters optimization problem:

- Three unknown parameters (p_0, p_1, and p_2) to describe the evolution of D_{self} (m^2/s) vs. ω_s:

$$D_{\text{self}} = \exp\left(\frac{p_1\omega_s + p_0}{\omega_s + p_2}\right); \tag{1}$$

- Two unknown parameters (p_3 and p_4) to get D_{SP} from D_{self}

$$D_{SP} = \left[\frac{(1-\varphi_s)(1-2\chi\varphi_s) + \varphi_s/p_4}{p_3\varphi_s^2 + (1-\varphi_s)(1+2\varphi_s)}\right] D_{\text{self}}, \tag{2}$$

where φ_s is the solvent volume fraction and χ is the Flory-Huggins interaction coefficient, which is assumed to be known in this study.

These five independent parameters are easily deduced from the theoretical expressions of D_{self} and D_{SP}. The advantage

Table 1. Error Estimation for Cubic Spline Parameterization

	Indices	0	1	2	3	4	5	6	7	8
1	ω_s	0	0.021	0.051	0.094	0.155	0.242	0.367	0.545	0.800
2	p_i	−13.49	−12.30	−11.30	−10.50	−9.89	−9.46	−9.20	−9.10	−9.23
3	$\lvert\Delta p_i\rvert$ with exact data	0.05	0.01	0.03	0.06	0.08	0.05	0.01	0.04	0.12
4	$\lvert\Delta p_i\rvert$ due to errors on q_j	0.15	0.04	0.1	0.02	0.16	0.03	0.02	0.12	0.3
5	$\lvert\Delta p_i\rvert$ due to meas. errors	0.05	0.01	0.007	0.003	0.002	0.001	0.002	0.003	0.006
6	Total $\lvert\Delta p_i\rvert$	0.2	0.05	0.1	0.02	0.16	0.03	0.02	0.12	0.3
7	Relative error on D_{sp}	0.6	0.1	0.3	0.05	0.4	0.07	0.05	0.3	1

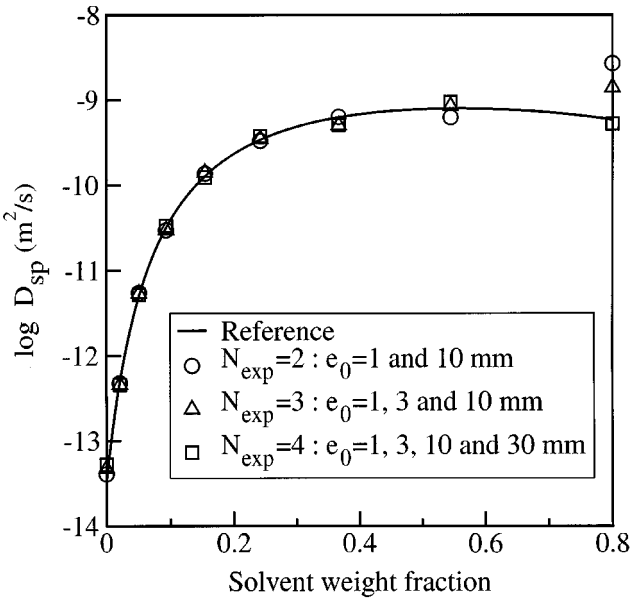

Figure 1. Estimation results, with uncertainty on h_m (−10%)— $h_m = h_{m_2} = 0.005$ m/s (cubic splines parameterization).

of this second parameterization is to use known physical knowledge on the behavior of diffusion coefficients. The dimension of the optimization problem is small, 5 parameters, that amounts to 3 as shown by a preliminary sensitivity study: as expected for polymer solutions, p_3 and p_4 affect the high dilution domain only, and can be assessed to arbitrary values in the problem under study (Doumenc et al., 1999). Its drawback, which is the counterpart of its advantage, is that it depends strongly on the validity of the theoretical model, which is not entirely validated in the case of the mutual-diffusion coefficient, especially for complex solutions. However, failing to find physical significance for the estimated parameters, the domain scanned by these equations may be thought large enough to include most of the diffusion laws, that is, Eq. 2 can be tested as a general-fit law.

For clarity, the results are detailed for the splines parameterization, which is more difficult to handle from the optimization point of view. A comparison with the parameterization based on the free-volume model is made at the end of the article.

Drying Model. Given the estimation of $D_{SP}(\omega_S)$ at the current iteration, the drying model calculates the mass evolution $m(t)$ corresponding to the test problem under study. This model must describe the diffusion of the solvent through the varnish layer, the moving interface, and the coupled heat and mass transfers between the interface and the drying air. The corresponding equations are given in Guerrier et al. (1998). The main assumptions of this drying model are the following: the solvent diffusion through the film is 1D and Fickian (rubbery state), and local thermodynamical equilibrium is assumed. The solution temperature, $T(t)$, is obtained by solving a thermal balance, taking into account solvent evaporation and exchange with the ambient air. The solvent partial pressure vapor depends both on temperature and solvent concentration, through the Flory-Huggins model. Since the estimation procedure requests the use of the drying model very frequently, it is crucial to optimize the CPU time. The resolution method uses a finite volume approach. A pure implicit time scheme was chosen because of its stability. Due to the important concentration gradient near the interface, and in order to limit the total number of finite volumes, an irregular grid based on a geometrical progression was used for space discretization. A Landau transformation was used to deal with the moving-boundary problem. The set of nonlinear algebraic equations issued from the finite volume discretization was solved at each time step by the Newton-Raphson algorithm.

Known Parameters. To test the validity of this estimation method thoroughly, we did a prior sensitivity study, in order to analyze the effect of all the parameters on the problem output, that is, the mass $m(t)$. Among these parameters, we consider not only the n unknown parameters $p_i\ (0 \le i \le n-1)$ corresponding to the parameterization of D_{SP} but also the *a priori* m known parameters $q_j\ (0 \le j \le m-1)$. Indeed, besides the mutual-diffusion coefficient, D_{SP}, several other parameters are involved in the drying model (Guerrier et al., 1998). They are assumed to be known in the estimation procedure, with some uncertainty. These q_j parameters are the following: $q^T = (T_a,\ h_{th},\ h_m,\ V_P,\ V_S,\ \chi)$, where T_a is the drying air temperature, h_{th} and h_m are the heat- and mass-transfer coefficient between the film interface and the drying air, V_P and V_S are the specific polymer and solvent volumes, and χ is the Flory-Huggins interaction parameter.

The uncertainties on the other parameters were shown to give a negligible outcome on the estimation of D_{SP}.

Criterion. The criterion to be minimized evaluates the relative distance between the measured mass, $M(t)$, and the mass obtained with the drying model, $m(p,q,t)$, for a given estimation of $D_{SP}(\omega_S)$, that is, a given vector of unknown parameters p:

$$J(p,q) = \sum_{l=1}^{N_{\text{exp}}} \sum_{k=1}^{K_l} \left[\frac{m_l(p,q,t_k) - M_l(t_k)}{M_l(t_k)} \right]^2 + R(p), \quad (3)$$

where $p = (p_0,\ p_1,\ \ldots,\ p_{n-1})^T$ and $q = (q_0,\ q_1,\ \ldots,\ q_{m-1})^T$; N_{exp} is the number of experiments; K_l is the number of measurements for the lth experiment; $\tau_l = t_{K_l}$ is the duration of the lth experiment; n is the dimension of the nonlinear optimization problem, with $n = 9$ or $n = 3$ when using the cubic splines parameterization or the free-volume parameterization, respectively; and $R(p)$ is a regularization term, usually used in estimation problems to increase the stability of the numerical procedure when the problem is badly conditioned. The regularization term introduces *a priori* knowledge on the behavior of the parameters to be estimated. In our problem, since we know that the mutual-diffusion coefficient varies little in the dilute domain, we consider the following regularization term:

$$R(p) = \alpha \rho_{S_0}^2 \int_{\omega_r}^{\omega_{S_0}} \left\{ \frac{\partial \left[\log D_{SP}(p,\omega_S) \right]}{\partial \rho_S} \right\}^2 d\omega_S, \quad (4)$$

where ρ_{S_0} and ω_{S_0} are the initial solvent concentration and weight fraction, respectively. The regularized domain is defined by $\omega_r \le \omega_S \le \omega_{S_0}$. In the following, the regularization weight, α, is zero except when explicitly said.

Minimization Algorithm. To minimize J, we used the Levenberg-Marquardt algorithm, which is a classic method for the nonlinear unconstrained optimization problem (Walter and Pronzato, 1997). This algorithm ensures a good compromise between robustness and rapidity. The method is iterative; the new estimation of the vector p at the iteration $it+1$ is deduced from the values of p, the gradient (first derivative), and the Hessian (second derivative) of J at the iteration it. The Hessian is estimated with the Gauss-Newton approximation. The numerical estimations of the gradient and the Hessian are performed with finite differences, and require several numerical resolutions of the drying model, which underlines the necessity to get a short CPU time for this model.

Several convergence tests are checked before stopping the iterative procedure: the gradient norm $\|\nabla J\|$, the criterion variation $|J^{(it+1)} - J^{(it)}|$, and parameter variation $\|p^{(it+1)} - p^{(it)}\|$ between the two last iterations must all be less than the given tolerances. One of the difficulties encountered during this optimization is the possible divergence of the drying model. Indeed, for some estimation of the vector p, the numerical resolution of the drying model fails. In that case, we use the specific strategy of the Levenberg-Marquardt algorithm. The relaxation factor of the algorithm is multiplied by ten and the procedure is reiterated from the previous iteration step. In addition, as often encountered in iterative optimization methods, the maximum value of the parameter variation between two iterations is bounded.

Test Problems

As was said in the Introduction, the analysis of the estimation procedure is not performed with real experimental mass measurements, but with virtual ones, obtained thanks to the simulation of various test problems. These test problems are close to the expected experimental conditions. Evaporation in ambient air of a polymer solution at room temperature is studied. The initial solvent weight fraction is 0.8 and the initial thickness lies between 1 and 30 mm. The order of magnitude of the heat- and mass-transfer coefficients are evaluated from experiments with pure solvent (Guerrier et al., 1998), in various configurations (diffusive or convective regimes). For the different configurations, good reproductibility was obtained experimentally in the determination of h_m ($\pm 10\%$) and h_{th} ($\pm 20\%$). In order to get the typical shape of D_{SP} vs. concentration in polymer solutions, we used the free volume model (cf. Table 1 and Figure 1). Toluene is the solvent.

The values of the q_j parameters are the following:

$$T_a = 20°C, \quad V_S = 1{,}15 \times 10^{-3}\ \text{m}^3/\text{kg}, \quad V_P = 0{,}97 \times 10^{-3}\ \text{m}^3/\text{kg},$$

$$\chi = 0.43 - 0.31(1-\varphi_S) - 0.036(1-\varphi_S)^2,$$

$$h_{th} = 100\ \text{W/m}^2/\text{K}.$$

(The heat-transfer coefficient expresses the thermal exchanges between the system and the environment. The main contribution is due to the thermal contact between the dish and the balance.)

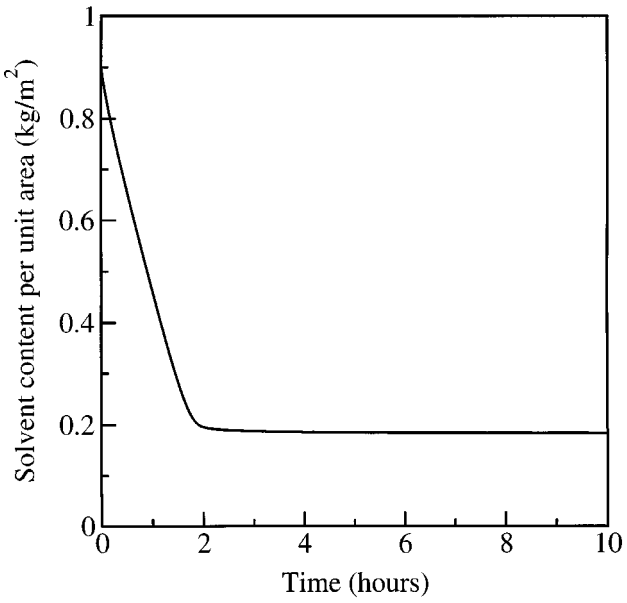

Figure 2. Simulation of the solvent content per unit area for: $e_0 = 1$ mm, $h_m = h_m(t)$ (Eq. 5).

Different mass-transfer coefficients have been considered: in the first case (h_{m_1}), the transfer in the ambient air, is assumed to be mainly diffusive. The time of establishment of the quasi steady state in the gas phase is taken into account through a time-variable mass-transfer coefficient $h_m(t)$ (t in seconds):

$$h_m(t) = h_{m_1} \times \left[1 + 0.406\exp\left(-t/10^3\right) + 0.255\exp\left(-4t/10^3\right) + 0.298\exp\left(-9t/10^3\right)\right], \quad (5)$$

with $h_{m_1} = 9.5 \times 10^{-4}$ m/s.

The two other cases (constant coefficients h_{m_2} and h_{m_3}) correspond to the convective regimes due to typical air velocity in a laboratory extractor hood: $h_{m_2} = 5 \times 10^{-3}$ m/s, $h_{m_3} = 10^{-2}$ m/s.

To illustrate a typical drying kinetics, we first present the drying simulation for the following test problem: $e_0 = 1$ mm, $\omega_{S_0} = 0.8$, $h_m = h_m(t)$. The time evolution of the solvent content per unit area and of the mass flux are given in Figures 2 and 3. This global mass evolution is the information used in the optimization procedure. Figure 4 shows the solvent weight fraction profile in the layer at different times (semilog scale), not reachable in our simple gravimetric experiments. As can be seen, the drying kinetics is characterized by two distinct regimes: in the first part, the solvent mass decreases rapidly. During this "fast" regime ($t \le 1$ h 45 min), the solvent weight fraction in the film and at the air/film interface is such that both the solvent activity and the diffusion coefficient are still quite high, so that important diffusion and evaporation flux take place. On the other hand, in the second part ($t > 1$ h 45 min), as the diffusion coefficient decreases significantly for solvent weight fraction smaller than 0.1 (cf. Figure 1), diffu-

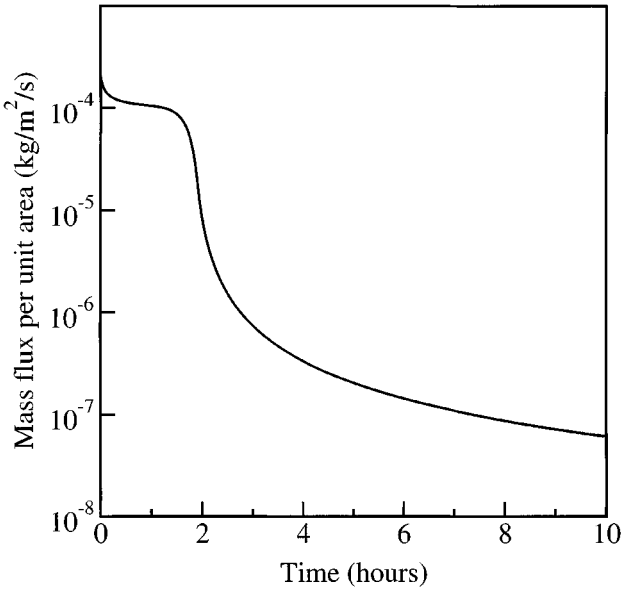

Figure 3. Simulation of the solvent mass flux.

Same configuration as Figure 2.

sion becomes too slow to allow sufficient regeneration of solvent at the interface. As a consequence, there is a large decrease in the mass flux and a strong concentration gradient appears in the film, as shown on Figures 3 and 4. The first regime is mainly driven by the transfers with the ambient air, while the slow regime kinetics is dominated by the solvent diffusion through the layer.

Experimental Strategy

This section deals with the definition of the experimental strategy required by the estimation problem: the objective is to get an estimation of the whole vector of the unknown parameters p, which is not very sensitive to the uncertainties on the *a priori* known parameters q.

To get reasonable experimental time, we limit the drying duration τ to 60 h for the whole study. Preliminary tests were made for the test problem described previously [Figure 2: $e_0 = 1$ mm, $\omega_{S0} = 0.8$, and $h_m = h_m(t)$]. With a horizon of 60 h, the solvent concentration at the end of the drying period is close to zero, so that the drying kinetics is sensitive to the diffusion coefficient $D_{Sp}(\omega_S)$ with ω_p varying from ω_{S_0} to 0. If no error is introduced in the identification process (that is, the uncertainties of the q_j parameters and the measurement errors are assumed to be negligible), the algorithm always converges toward the exact solution, whatever the initial estimation D_{SPO} (D_{SP_0} constant $= 10^{-13}$ m^2/s or 10^{-9} m^2/s).

In a second step, we took into account the uncertainties on the q_j parameters by introducing an error of 10% on the mass-transfer coefficient, which is one of the key parameters that control the first regime. With the introduction of such an error, the estimation completely failed, whatever the parameterization and the initial estimation. That is why an accurate analysis is needed to elaborate an experimental strategy suitable for our estimation problem.

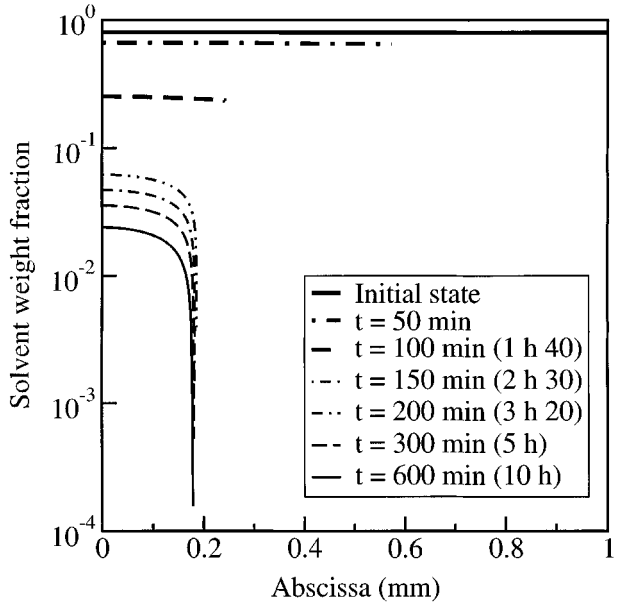

Figure 4. Simulation of the solvent weight fraction profile.

Same configuration as Figure 2.

Sensitivity function analysis

In order to get a better understanding of the main difficulties of the estimation, the behavior of various sensitivity functions was thoroughly analyzed. The sensitivity function of the model output to the unknown parameter p_i is defined as

$$Q_{p_i}(p,q,t) = \frac{|p_i|}{m(p,q,t)} \frac{\partial m(p,q,t)}{\partial p_i}. \qquad (6)$$

Because of the absolute value, $|p_i|$, the sensitivity function and the derivative of the model output have like signs. The sensitivity functions for the known parameters q_j are defined in the same way. Before analyzing the behavior of the sensitivity functions of this estimation problem, let us recall some general points. Suppose the sensitivity function associated with a given parameter is very small compared to another, on the overall time range of the experiments, the effect of this low-sensitivity parameter will be hidden by the large one, and the problem will be ill-conditioned. In the similar way, if some of the sensitivity functions are ''almost'' linearly dependent on the overall horizon, different sets of parameters give almost the same model output (ill-conditioned problem).

Let us now consider the sensitivity functions computed with $e_0 = 1$ mm, $\omega_{S_0} = 0.8$, and $h_m = h_m(t)$ (Figure 5). The higher the sensitivity function's absolute value, the higher the effect of the parameter on the model output. The maximum of Q_{hm} is obtained at $t = 1$ h 36 min. For $t \leq 2$ h, the Q_{p_i} (that is, the effect of the diffusion coefficient) are very weak, compared to Q_{h_m}: Q_{p_6}, Q_{p_7}, and Q_{p_8}, which correspond to high ω_S, are one order of magnitude smaller than Q_{h_m}. After this delay, we turn to the opposite situation: Q_{h_m} rapidly decreases and becomes smaller than $Q_{p_i,\ i \leq 3}$. This is a consequence of the

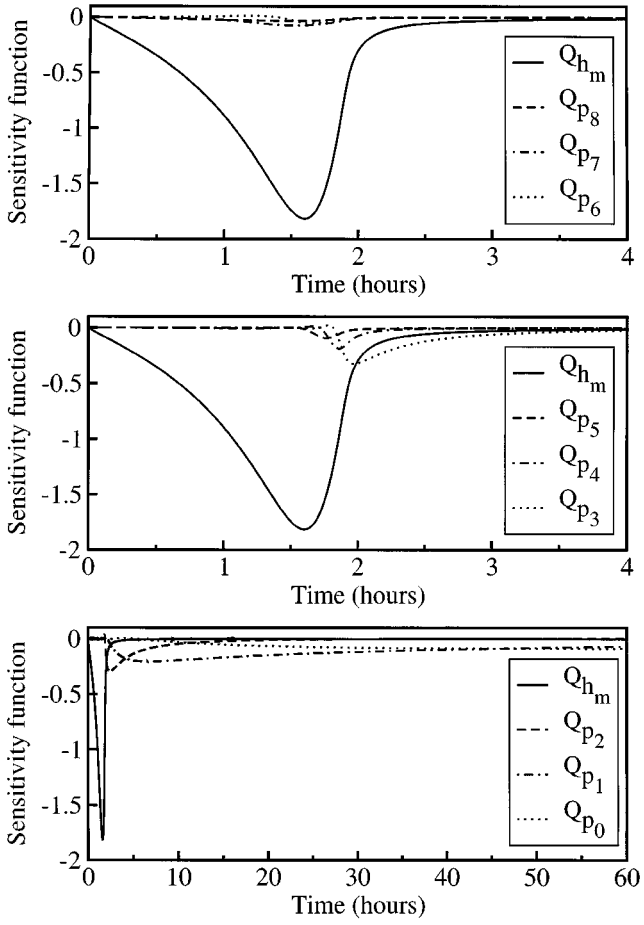

Figure 5. Sensitivity functions for: $e_0 = 1$ mm, $h_m = h_m(t)$.

For clarity, the variations obtained for the various Q_{p_i} are drawn on separate graphs.

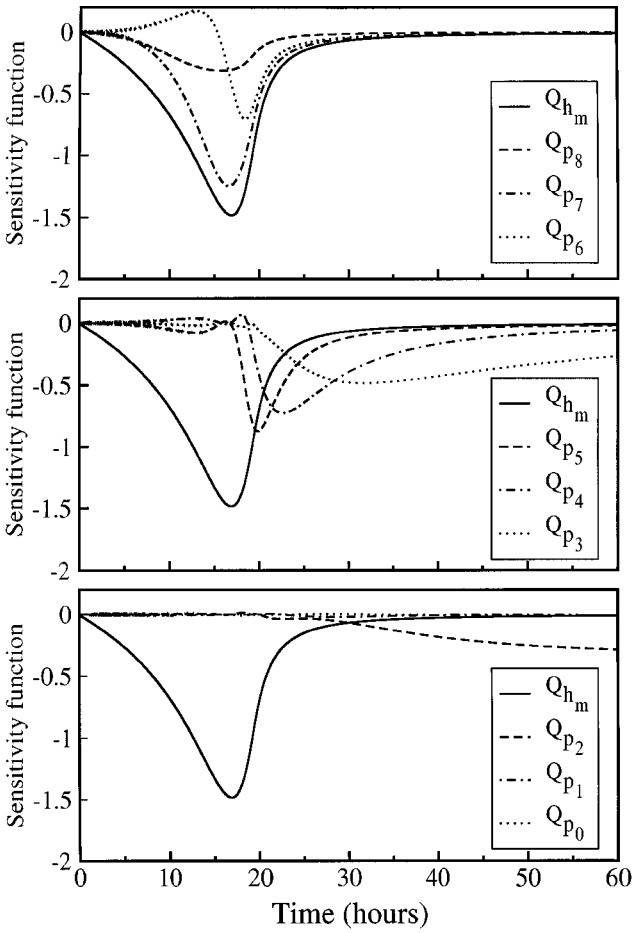

Figure 6. Sensitivity functions for: $e_0 = 10$ mm, $h_m = h_m(t)$.

two regimes described previously: the evaporation process is first driven by the solvent transfer in the air above the solution, described by h_m, and is then driven by the diffusion. That is the reason why the algorithm is not robust to a little perturbation on h_m in the experimental configuration used in the preliminary test. Indeed, a small error on h_m leads to a large error on the parameters describing D_{sp} in the dilute domain, since the minimization algorithm tries to balance the error on h_m and to fit the experimental data, thanks to D_{sp}.

At this stage of the sensitivity study, one can conclude that the experimental conditions must be chosen so that the mass transfer in the gas phase does not conceal the diffusion in the high solvent concentration domain corresponding to the beginning of the drying. To modify the kinetics of this first regime, one can change various parameters: the initial thickness, the mass-transfer coefficient, and the initial solvent concentration. Figure 6 shows the sensitivity functions computed with the initial thickness multiplied by ten [$e_0 = 10$ mm, $\omega_{S0} = 0.8$, $h_m = h_m(t)$]. The parameters corresponding to the dilute domain— p_8 excepted—now exhibit sensitivity functions close to Q_{h_m}. This result is in agreement with what we are looking for. Another promising result lies in the change in the positions of the Q_{p_i}: the distance between the extrema increases, so that there is no linear dependence between the functions Q_{p_7} to Q_{p_2}; each parameter p_i controls a part of the drying curve. Indeed, as drying progresses, the concentration decreases and the p_i, which correspond to different solvent mass fractions, dominate one after the other.

Despite the undeniable improvement brought by switching the initial thickness from 1 mm to 10 mm, all the difficulties are not solved, as shown, for example, in Figure 6. First, Q_{p_8} is still small compared to Q_{h_m}, and a quasi linear dependence between Q_{p_8} and Q_{p_7} can be suspected. Moreover, and this point is the most critical, Q_{p_1} and Q_{p_0} are close to zero in the entire time range, so that they cannot be estimated from this experiment. This is due to the experimental horizon chosen, $\tau = 60$ h, which is not sufficient for the concentrated domain to be explored. Let us emphasize that, since the diffusion characteristic time is inversely proportional to e^2, the required experimental time should be at least several weeks. We conclude that to get enough information on the entire concentration domain, several experiments have to be performed, with different initial thicknesses. Experiments on small and large thicknesses give information on the concentrated and dilute domain, respectively. This approach will be tested by numerical simulations in the next section.

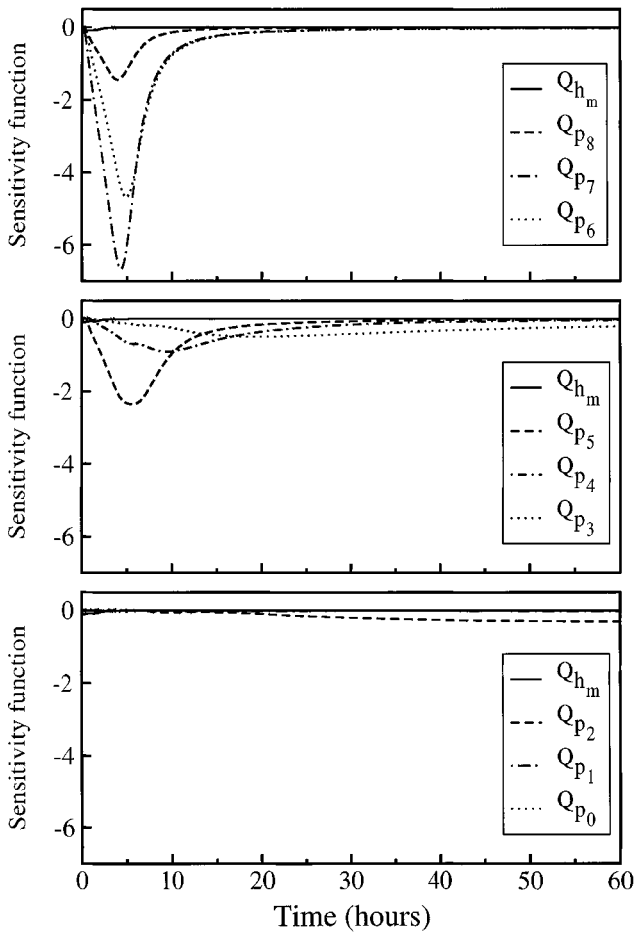

Figure 7. Sensitivity functions for: $e_0 = 10$ mm, $h_m = h_{m_3} = 0.01$ m/s.

The second parameter to be investigated in the sensitivity study is the mass-transfer coefficient h_m. The sensitivity functions shown in Figure 7 were computed with a mass-transfer coefficient about one order of magnitude higher ($h_{m_3} = 0.01$ m/s, $e_0 = 10$ mm, and $\omega_{S_0} = 0.8$). Increasing h_m makes the solvent transfer in the gas phase easier, so the duration of the first regime is smaller. As a consequence, the sensitivity functions of the parameters describing the diffusion coefficient in the dilute domain (Q_{p_8} to Q_{p_6}) are much larger than Q_{h_m}, which is close to zero on the overall time horizon. On the other hand, the sensitivity functions corresponding to the concentrated domain (Q_{p_3} to Q_{p_0}) are weakly modified by a change in h_m. This confirms and completes the conclusion already pointed out: multiple experiments with different initial thicknesses are needed to get information on the whole concentration domain. Moreover, increasing h_m leads to a much better estimation in the dilute domain. Then one could expect that most of the difficulties are solved by a suitable experimental strategy, except the quasi linear dependence between Q_{p_7} and Q_{p_8}.

The initial solvent weight fraction ω_{S_0} is the last parameter investigated. Qualitatively, ω_{S_0} has the same effect on the sensitivity functions as e_0. For a given experimental horizon, the sensitivity functions in the dilute (concentrated) domain increases (decreases) when ω_{S_0} decreases. However, for practical reasons, it is not possible to decrease the initial solvent concentration a great deal, since the solution viscosity would increase too much. Moreover, decreasing ω_{S_0} leads to a restriction of the concentration domain covered by the identification. For these reasons, we assessed a value of 0.8 to ω_{S_0} throughout the present study.

Estimation with multiple drying experiments

In the second step, the conclusions obtained from the sensitivity study on the required experimental strategy were confirmed by numerical simulations. First, whatever the number of experiments (up to five, with $e_0 = 1$, 3, 10, 30, and 100 mm), the optimizations corresponding to the mass-transfer coefficient $h_m(t)$ (mainly diffusive regime) failed as soon as an error of 10% was introduced on h_{m_1}. Simulations were then performed with h_{m_2} (convective regime), for various experimental configurations: $2 \le N_{\text{exp}} \le 4$ and $1 \le e_0 \le 30$ mm. Except for the "$N_{\text{exp}} = 2$, $e_0 = 1$, and 3 mm" case, the convergence of the optimization algorithm was obtained for all the tested configurations. The corresponding results are shown on Figure 1. As expected, the effect of the uncertainty on h_m is mainly located in the dilute domain. It decreases when greater thicknesses are taken into account. With a mass-transfer coefficient that is two times higher, $h_m = h_{m_3}$, convergence was obtained, even for the configuration "$N_{\text{exp}} = 2$, $e_0 = 1$, and 3 mm," but with a large error at $\omega_S = 0.8$. The other configurations led to very good results, close to the reference solution.

Algorithm Robustness

Methodology

The previous results have shown the feasibility of the estimation method, provided a suitable experimental strategy is performed. In this last section, we study the robustness of the proposed algorithm, and we thoroughly analyze the consequences of all the errors that may affect the optimization process:

- *Modelization errors:* Some assumptions that could be partly invalidated in a real experiment have been made in building the drying model (Guerrier et al., 1998). This point is not studied in this article; however, some of the assumptions are taken into account indirectly through the errors on the known parameters q. For example, the uncertainty about the mass transfer h_m may correspond partly to an invalidation of the assumption of a spatially uniform coefficient.
- *Numerical errors:* These errors come from the numerical resolution of the drying model. A preliminary study has been done in order to choose a spatial grid and a time step small enough to make these errors negligible.
- *Parameterization errors, due to the modelization of D_{SP} by a given curve, with a finite number of parameters, p_i:* This error can easily be neglected in the spline parameterization, by setting enough interpolation points. In the free-volume parameterization, the possible error is inherent in the choice of this model.
- *Errors on the known parameters q_j:* For each parameter q_j, a range of variation has been estimated, with $q_{j_{\min}} \le q_j \le$

Table 2. q_j Parameters for Tests 1 and 2

Test Case	h_m (%)	h_t (%)	θ (°C)	χ	V_s (%)	V_p (%)
1	+10	+20	+0.2	$\chi = 0.5$	−3	−6
2	−10	−20	−0.2	$\chi = 0$	+3	+6

$q_{j_{\max}}$. The "true" q_j (that is, the q_j used to build the virtual experimental data) is the mean value, except for the Flory interaction parameter χ: the virtual data were built with an interaction parameter χ that varies with the solvent concentration (cf. the test problem section), and the error analysis was performed with a constant χ ($0 \le \chi \le 0.5$). Then, for each parameter, the estimation was performed with $q_j = q_{j_{\min}}$ and $q_j = q_{j_{\max}}$ with the following configuration: $h_m = h_{m_3}$, $N_{\exp} = 3$, and $e_0 = 1$, 3, 10 mm. Finally, we defined two tests with cumulative errors: for each parameter q_j, we chose the bound ($q_{j_{\min}}$ or $q_{j_{\max}}$) that underestimates D_{SP} (test 1) or, just opposite, overestimates D_{SP} (test 2). Errors on χ, V_s, and V_p were estimated from dispersion of data from the literature, while errors on h_m and h_{th} came from the reproducibility analysis of drying experiments with pure solvent. The values corresponding to these two tests are given in Table 2.

• *Measurement errors:* The usual assumptions have been made for the description of the measurement errors. They are modelized by white Gaussian noise, with constant standard deviation (10 mg, which leads to a standard deviation of 2 g/m^2 in the test problem under study). The corresponding uncertainties on the parameters p_i are deduced from the Fischer matrix. Let us notice that, since the standard deviation is constant, we should have used an absolute criterion instead of a relative one, in the sense of the maximum likelihood (Walter and Pronzato, 1997). The uncertainties evaluated with the two criteria are very similar. That is why we have used a relative criterion in this study; it is more stable from the numerical point of view. Since these uncertainties change very little when q_j varies, the total uncertainty is estimated by adding the two components (that is, the uncertainties induced by the errors on the parameters q_j and by the measurement errors). Finally, to make sure that these random errors do not affect the convergence of the algorithm, some simulations have been made with noisy data, obtained by adding white Gaussian noise to the virtual data of the test problem.

Error estimation

The results of the first test (cf. Table 2) are given in Figure 8. As can be seen, without regularization, the estimation is very accurate in the concentrated domain, but large oscillations appear in the dilute domain (circle symbol), though all the convergence criteria are satisfied. These oscillations do not appear when only one parameter q_j is perturbed, and are due to the cumulative effects of the errors on all the q_j. A more detailed analysis shows that this phenomenon is due to the poor condition number of the Hessian, which is about 10^{-6}. This can be correlated to the "almost" linear dependence of the sensitivity functions Q_{p7} and Q_{p_8} (Figure 7).

As previously noted, we add a regularization term to the criterion to overcome this problem (cf. Eqs. 3 and 4). The choice of the optimal regularization weight, α, is a tricky

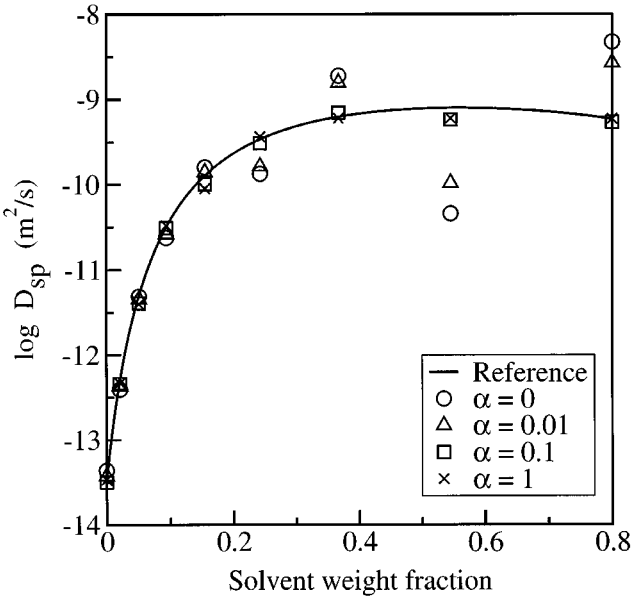

Figure 8. Estimation results: influence of the regularization weight α—test 1 (cubic splines parameterization).

problem in nonlinear optimization. We set α empirically by increasing it until the oscillations are almost eliminated. We also checked that an accurate determination of the regularization parameters, α and ω_r, is not needed. This is illustrated in Figure 8: the value $\alpha = 0.01$ is clearly too weak, while the results obtained with $\alpha = 0.1$ or 1 are satisfactory. The Hessian condition number is now 6×10^{-5}, and the regularization term $R(p)$ is about 1% of the total criterion $J(p, q)$. The influence of the size of the regularized domain has also been investigated. Qualitatively, similar results are obtained with $\alpha = 1$, $\omega_r = 0.3$, and $\alpha = 10$, $\omega_r = 0.6$.

Finally, the same test was performed with noisy measurements, with no change in the results. Concerning the second test (cf. Table 2), the estimation was easier, since no oscillations appeared. Results with or without regularization, and with or without noisy measurements are similar and very close to the reference solution.

These results are summed up in Figure 9 and Table 1, which gives the uncertainty of the estimated p_i due to the various errors considered. These results correspond to the regularized criterion, with $\alpha = 1$ and $\omega_r = 0.3$. The two first lines give the abscissa and ordinate of the reference p_i used to generate the "virtual" experimental data. Line 3 corresponds to the optimal case, with no measurement errors and true values of q_j. The estimated solution in very close to the reference one. The fourth line gives the maximal error obtained with test 1 or 2. Line 5 corresponds to the 95% confidence band due to the measurement errors, and deduced from the Fischer matrix. The effect of measurement errors is weak, as confirmed by simulations with noisy data. Finally, lines 6 and 7 give the total error on p_i and the magnitude of the relative error on D_{SP}: $|D_{\text{ref}} - D_{\text{estimated}}|/D_{\text{ref}}$. The accuracy is good in the whole concentration domain, with a relative error of less than one, while D_{SP} varies by about four orders of magnitude. Let us notice that, for the test problem under study,

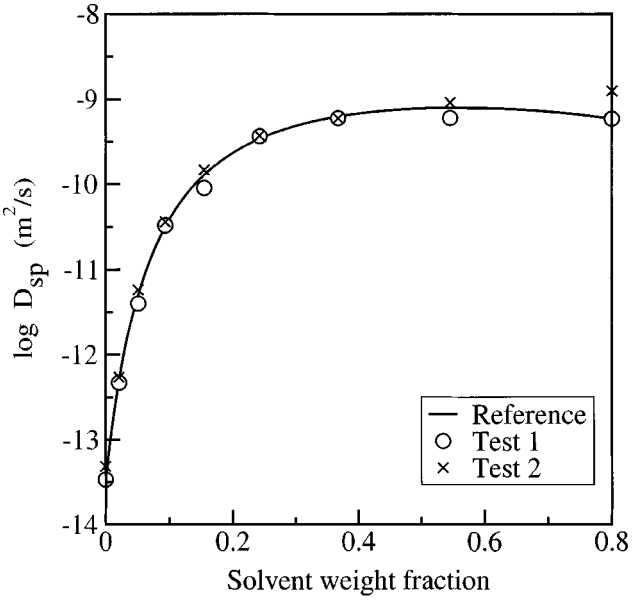

Figure 9. Estimation results for tests 1 and 2—noisy measurements (cubic splines parameterization).

these results were quite easily obtained for the concentrated domain, while the diluted domain was more difficult to handle, as expected from the sensitivity study. As shown in Figure 10, the output error is mainly located at the beginning of the drying, when the kinetics still depends on the mass-transfer coefficient, h_m.

These results have been obtained for various initial estimations D_{SP_0} constant $\in [10^{-11}, 10^{-8}$ m^2/s]. The CPU time depends on the initial estimation, and is about 20 to 40 h with a workstation IBM RS6000 Power 2.

Free-Volume Parameterization

The same methodology was used to analyze the behavior of the estimation method, with the free-volume parameterization. The sensitivity study leads to the same experimental strategy. Most of the results are qualitatively similar, so we do not cite the whole study and focus on the errors analysis. Estimation results for tests 1 and 2 are given in Figures 11 and 12. The relative difference between the reference and estimated diffusion coefficient is always less than one, as with the spline parameterization. As previously, the errors on the estimated p_i due to measurement errors were found negligible compared to the one due to uncertainty on the q_j. This was confirmed by simulations with noisy data.

Let us emphasize that this parameterization is more "robust," in the sense that no regularization is needed, since the shape of the estimated function is defined by the parameterization. Moreover, the CPU time is two or three times smaller than with the splines parameterization.

Conclusion

In this study, an optimization method coupled with very simple gravimetric experiments was shown to give an accurate estimation of the mutual-diffusion coefficient, $D_{SP}(\omega_S)$, on a large concentration domain ($0 \le \omega_S \le 0.8$), and especially in the concentrated domain. The sensitivity of the method to various errors (namely, measurement errors and

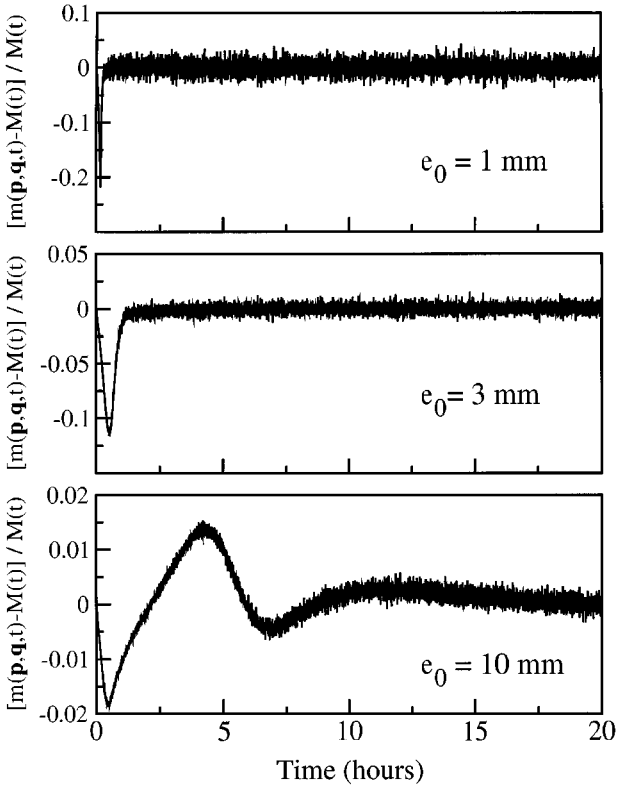

Figure 10. Model output error—test 1 (cubic splines parameterization).

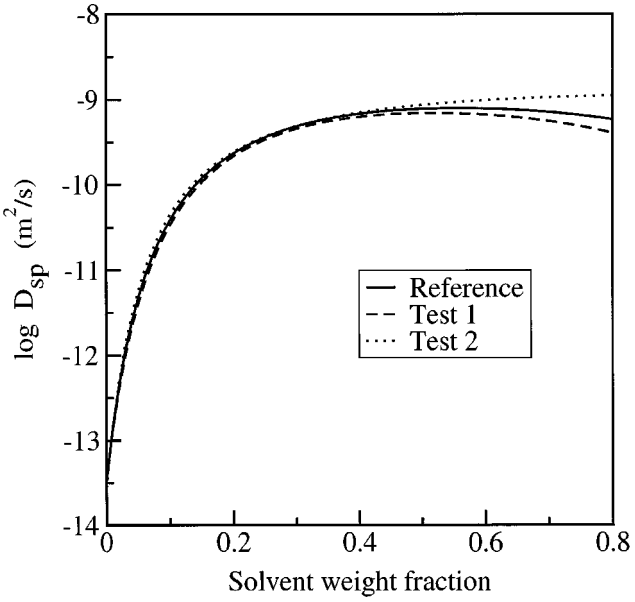

Figure 11. Estimation results for tests 1 and 2—noisy measurements (free volumes parameterization).

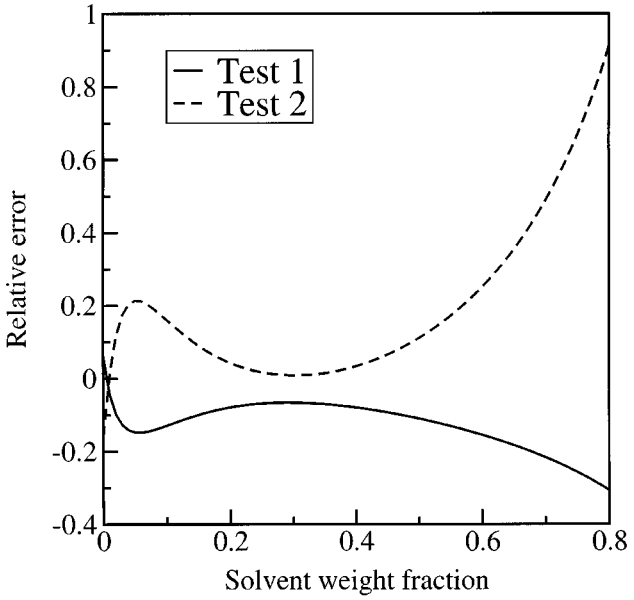

Figure 12. Relative error on D_{SP} (free volumes parameterization).

uncertainties on *a priori* known parameters) has been investigated. The method is robust, provided a suitable experimental strategy is used. Indeed, the various analyses performed have stressed the great sensitivity of the estimation procedure to the parameters that characterize the transfer between the interface and the drying air. This difficulty may be overcome by coupling several experiments with different thicknesses, and by having a high mass transfer coefficient. On the other hand, the estimation is not sensitive to random measurements errors. Two parameterizations of the mutual diffusion coefficient $D_{SP}(\omega_S)$ have been compared: the first one uses cubic splines; the second one uses the free-volume theory. The first parameterization is more general, but the second one is easier to handle, since it contains implicit regularization. From the numerical point of view, it was crucial to minimize the CPU time of the drying model and to ensure its stability, in order to limit the total CPU time of the estimation procedure, which is still more than 10 h. In the next step of this study, the estimation method will be tested on real experimental data, obtained using the experimental strategy defined in this article.

Acknowledgments

This work was supported by PEFE (Pechiney Emballage Flexible Europe). The authors gratefully thank E. Walter (Lab. des Signaux et Systèmes, France) for helpful discussions. The numerical calculations have been performed on the computers of the ''Centre National de Calcul'' of CNRS (IDRIS), and of the ''Centre de Calcul Recherche'' of the University Pierre et Marie Curie (Paris).

Literature Cited

Bandis, A., P. T. Inglefield, A. A. Jones, and W. Y. Wen, ''A Nuclear Magnetic Resonance Study of Dynamics in Toluene-Polyisobutylene Solutions,'' *J. Poly. Sci., Part B: Poly. Phys.*, **33**, 1495 (1995).

Billovits, G. F., and C. J. Durning, ''Linear Viscoelastic Diffusion in the Poly(styrene)-Ethylbenzene System: Differential Sorption Experiments,'' *Macromol.*, **26**, 6927 (1993).

Blum, F. D., and S. Pickup, ''Solvent Self-Diffusion in Polystyrene-Solvent Systems,'' *J. Coatings Technol.*, **59**, 53 (1987).

Bouchard, C., B. Guerrier, C. Allain, A. Laschitsch, A. C. Saby, and D. Johannsmann, ''Drying of Glassy Polymer Varnishes: A Quartz Resonator Study,'' *J. Appl. Poly. Sci.*, **69**, 2235 (1998).

de Gennes, P. G., *Scaling Concepts in Polymer Physics*, Cornell Univ. Press, Ithaca, NY (1979).

Deppe, D. D., R. D. Miller, and J. M. Torkelson, ''Small Molecule Diffusion in a Rubbery Polymer Near tg: Effects of Probe Size, Shape and Flexibility,'' *J. Poly. Sci., Part B: Poly. Phys.*, **34**, 2987 (1996).

Doumenc, F., B. Guerrier, and A. C. Saby, ''Estimation du Coefficient de Diffusion Mutuelle Solvant/Polymere,'' *Proc. Congrès SFT 99 Thermique et Matériaux*, Elsevier, Amsterdam, p. 569 (1999).

Frick, T. S., W. J. Huang, M. Tirrell, and T. P. Lodge, ''Probe Diffusion in Polystyrene/Toluene Solutions,'' *J. Poly. Sci., B: Poly. Phys.*, **28**, 2629 (1990).

Guerrier, B., C. Bouchard, C. Allain, and C. Benard, ''Drying Kinetics of Polymer Films,'' *AIChE J.*, **44**, 791 (1998).

Hong, S. U., T. A. Barbari, and J. M. Sloan, ''Diffusion of Methyl Ethyl Ketone in Polyisobutylene: Comparison of Spectroscopic and Gravimetric Techniques,'' *J. Poly. Sci., B: Poly. Phys.*, **35**, 1261 (1997).

Lodge, T. P., J. A. Lee, and T. S. Frick, ''Probe Diffusion in Poly (vinyl acetate)/Toluene Solutions,'' *J. Poly. Sci., Part B: Poly. Phys.*, **28**, 2607 (1990).

Lohfink, M., and H. Sillescu, ''Tracer Diffusion in Polymer and Organic Liquids Close to the Glass Transition Studied by Forced Rayleigh Scattering,'' *Prog. Colloid Poly. Sci.*, **91**, 31 (1993).

Neogi, P., *Diffusion in Polymers*, Dekker, New York (1996).

Pickup, S., and F. D. Blum, ''Self-Diffusion of Toluene in Polystyrene Solutions,'' *Macromol.*, **22**(10), (1989).

Vrentas, J. S., and C. M. Vrentas, ''A New Equation Relating Self-Diffusion and Mutual-Diffusion Coefficients in Polymer Solvent Systems,'' *Macromol.*, **26**, 6129 (1993).

Vrentas, J. S., and C. M. Vrentas, ''Predictive Methods for Self Diffusion and Mutual Diffusion Coefficients in Polymer-Solvent Systems,'' *Eur. Poly. J.*, **34**, 797 (1998).

Waggoner, R. A., F. D. Blum, and J. M. D. MacElroy, ''Dependence of the Solvent Diffusion Coefficient on Concentration in Polymer Solutions,'' *Macromol.*, **26**, 6841 (1993).

Walter, E., and L. Pronzato, *Identification of Parametric Models from Experimental Data*, Springer-Verlag, London (1997).

Wisnudel, M. B., and J. M. Torkelson, ''Small-Molecule Probe Diffusion in Polymer Solutions: Studies by Taylor Dispersion and Phosphorescence Quenching,'' *Macromol.*, **29**, 6193 (1996).

Zielinski, J. M., G. Heuberger, H. Sillescu, U. Wiesner, A. Heuer, Y. Zhang, and H. W. Spiess, ''Diffusion of Tracer Molecules Within Symmetric Diblock Copolymers,'' *Macromol.*, **28**, 8287 (1995).

Zielinski, J. M., and B. F. Hanley, ''Practical Friction-Based Approach to Modeling Multicomponent Diffusion,'' *AIChE J.*, **45**, 1 (1999).

Zielinski, J. M., ''An Alternate Interpretation of Polymer/Solvent Jump Size Units for Free-Volume Diffusion Models,'' *Macromol.*, **29**, 6044 (1996).

Manuscript received Dec. 14, 1999, and revision received Oct. 3, 2000.